

## Photodegradation of Novel Nitromethylene Neonicotinoids with Tetrahydropyridine-Fixed Cis Configuration in Aqueous Solution<sup>†</sup>

XIANFENG ZHAO, XUSHENG SHAO, ZHUYAN ZOU, AND XIAOYONG XU\*

Shanghai Key Laboratory of Chemical Biology, School of Pharmacy, East China University of Science and Technology, Shanghai 200237, China

Photodegradation of 1-((6-chloropyridin-3-yl)methyl)-7-methyl-8-nitro-1,2,3,5,6,7-hexahydroimidazo[1,2-*a*]pyridin-5-ol (**IPPA152001**) and 1-((6-chloropyridin-3-yl)methyl)-7-methyl-8-nitro-5-propoxy-1,2,3,5,6,7-hexahydroimidazo[1,2-*a*]pyridine (**IPPA152004**) was studied in distilled water; high-pressure mercury lamp and xenon lamp were used as light sources. The photolytic rate constants of the two compounds and their half-lives were calculated. Compared with imidacloprid, the order of photodegradation rate of three compounds was as follows: imidacloprid > **IPPA152001** ≥ **IPPA152004**. Mercury lamp light intensity was measured with chemical actinometers. The quantum yields for photodegradation of **IPPA152001** and **IPPA152004** in distilled water were also calculated. Photodegradation products of **IPPA152004** were preliminarily identified on the basis of the spectral data of GC-MS, LC-TOF-ESI, and LC-MS-MS in positive mode. The photodegradation pathways of **IPPA152004** were proposed according to the structures of photoproducts.

**KEYWORDS:** Photodegradation; neonicotinoids; insecticide; cis configuration

### INTRODUCTION

The impact of using numerous insecticides on the environment has attracted more attention. After insecticides are sprayed on a field, various degradation processes are undergone, such as microbial degradation, hydrolysis, and photodegradation, which plays a key role in the degradation of pesticides because of its strong absorption in the near-ultraviolet or visible light range (1). Some photodegradation products may have undesirable negative effects on the environment and human health (2–5). To acquire environmental information on insecticides, it is urgent to study the photodegradation of insecticides in an aquatic environment.

Neonicotinoids are the fastest growing class of insecticides in modern crop protection for their high insecticidal activity, broad insecticidal spectra, low mammalian and aquatic life toxicity, good systemic properties, and suitable field stability (6, 7). They are used widespread against a broad spectrum of sucking and certain chewing pests acting selectively on insect nicotinic acetylcholine receptors (nAChRs) (7). Several groups have reported their results on photodegradation in aqueous solutions and soil of neonicotinoids such as imidacloprid, which is the most prominent member of the neonicotinoids, and thiacloprid (8–13). Furthermore, investigations of the effect of pH and photocatalysis TiO<sub>2</sub> and O<sub>3</sub> on the photodegradation of neonicotinoids as well as studies of the photodegradation of neonicotinoids in a nonaqueous environment have also been reported (14–17).

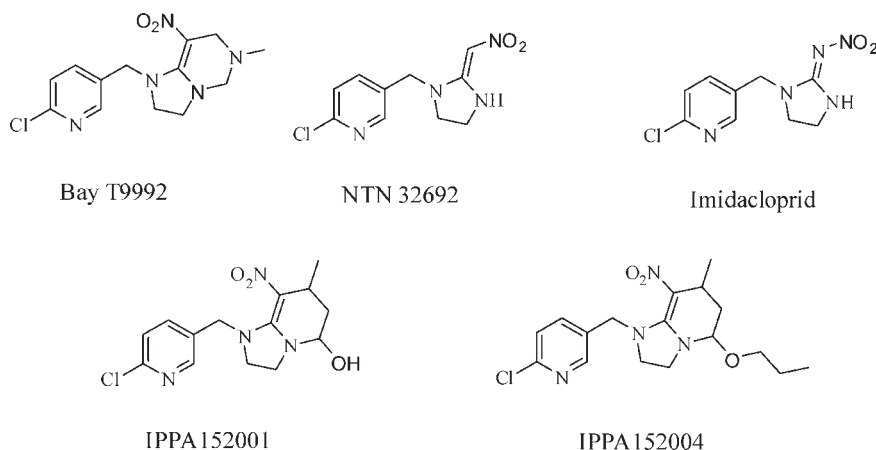
It is well-known that the –NO<sub>2</sub> group in imidacloprid is a pharmacophore and plays an important role in its activities.

The X-ray crystallographic study of imidacloprid by Kagabu showed that the *trans E* isomer, in which the nitro group is located in the *trans*-position, was predominant (18). Interestingly, Bayer introduced a tetrahydropyrimidine ring into the lead compound to fix the nitro moiety in the *cis*-position (**Bay T9992**) (**Scheme 1**), and the compound also showed high biological activity. However, it had high toxicity for mammals and aquatic life (19). On the basis of the study above, various neonicotinoid compounds with *cis*-nitro configuration were synthesized in our previous research (20, 21), whereas (2-chloro-5-((2-nitromethylene)imidazolidin-1-yl)methyl)pyridine (**NTN32692**) (**Scheme 1**) was used as a key intermediate. Bioassays indicated that some of the compounds exhibited high biological activity, especially for strains resistant against imidacloprid. As a prior consideration, **IPPA152004** has been defined as the trade name of Paichongding, which showed higher activities against imidacloprid-resistant brown planthopper than imidacloprid. Importantly, it also exhibited obvious interacting differences with the binding site of imidacloprid (22). It will be commercialized soon after possession of a Temporary Registration License in China (31).

With the wide application of imidacloprid, the problems of resistance and cross-resistance are becoming more and more striking for neonicotinoids with similar structures and modes of action (23, 24). Thus, neonicotinoids with *cis* configuration might gradually exhibit interesting influence on pest control. However, there was no report about the photodegradation of the *cis* configuration compounds. Therefore, it was essential to investigate the photodegradation of novel neonicotinoid compounds with a *cis*-nitro configuration for further scientific investigation such as environmental residence risk, ecotoxic relevance, and degradation products.

<sup>†</sup>Part of the ECUST-Qian Pesticide Cluster.

\*Corresponding author (telephone + 86-21-64253540; fax +86-21-64252603; e-mail xyxu@ecust.edu.cn).

**Scheme 1.** Chemical Structures of the 1,2,3,6-Tetrahydro-5-nitropyrimidine Derivatives (**C1**) NTN32692, Imidacloprid, **IPPA152001**, and **IPPA152004**

Herein, the kinetics of the photochemical degradation of **IPPA152001** and **IPPA152004** (Scheme 1) in aqueous solutions compared with imidacloprid were studied, the analysis of photo-degradation products was carried out, and the proposed photo-degradation mechanism was presented.

## MATERIALS AND METHODS

**Samples and Reagents.** All of the solvents used were of HPLC grade. Distilled water was used. The imidacloprid was procured from Kwin Co., Ltd., and crystallized from acetone. The standard sample *cis*-configuration neonicotinoids **IPPA152001** and **IPPA152004** were synthesized by ourselves according to the description in the literature (25). The purity of the compounds was determined to be >99.0%.

**Analytical Instruments.** A Bruker AM-400 (400 MHz) spectrometer was used with DMSO-*d*<sub>6</sub> or CDCl<sub>3</sub> as the solvent and TMS as the internal standard. Chemical shifts were reported in  $\delta$  (parts per million) values. High-resolution mass spectra were recorded under electron impact (70 eV) condition using a MicroMass GCT CA 055 instrument. The remains of the three compounds during the photodegradation process were estimated by HPLC. An Agilent 1200 series liquid chromatograph was equipped with a Zorbax XDB-C18 column (250 mm  $\times$  4.6 mm, particle size = 5  $\mu$ m), quarter pump, and a diode array detector. GC-MS analysis used an Agilent 7890A gas chromatograph with mass selective detector model 5975C (Palo Alto, CA) equipped with an HP-5MS (5% diphenyl-95% methylsiloxane) capillary column (30 m  $\times$  0.32 mm  $\times$  0.25  $\mu$ m). Ultraviolet spectra were measured with a Varian Cary 100 Bio spectrophotometer (Varian, Germany). The LC-TOF-ESI system consisted of an Agilent 6210 TOF-MS (Agilent Technologies, Palo Alto, CA). LC-MS/MS analysis was carried out by a Waters Acquity Ultra performance LC system with micro-mass Quattro micro API/ESCI multimode-ionization mass selective detector.

**Photolysis Experiments.** The photodegradation of imidacloprid, **IPPA152001**, and **IPPA152004** was conducted in an XPA series merry-go-round photochemical reactor (Xujiang Machine Factory, Nanjing, China) equipped with a 300 W high-pressure mercury lamp and a 500 W xenon lamp. The working current of 300 W high-pressure mercury lamp was 2.2 A and the operating voltage was 138.1 V; the working current of the 500 W xenon lamp was 6.4 A and the operating voltage was 75.6 V. The relative energies of the mercury lamp (not including infrared) and xenon lamp are listed in the Table 1. (The data were supplied by Xujiang Machine Factory.) The irradiation experiments were carried out with a water-cooled immersion wall. To investigate the influence of sample concentration on the degradation kinetics, imidacloprid, **IPPA152001**, and **IPPA152004** were dissolved in distilled water, respectively, and 40 mL of imidacloprid, **IPPA152001**, and **IPPA152004** aqueous solution ( $1 \times 10^{-5}$  and  $5 \times 10^{-5}$  mol L<sup>-1</sup>) contained in quartz cylindrical tubes (50 mL and 20 cm in height) were prepared and irradiated with the 300 W high-pressure mercury lamp. Dark control experiments were carried out at conditions similar to those described above, except that the tube was covered by aluminum foil. Aliquots of 2 mL irradiated solutions and control solutions were taken out at appropriate intervals and stored at 4 °C in the dark, and then analyzed by HPLC to monitor the peak area changes

**Table 1.** Chief Wavelength and Relative Energy of 300 W High-Pressure Mercury Lamp and 500 W Xenon Lamp

light source	wavelength (nm)	relative energy (%)
300 W high-pressure mercury lamp	265.2–265.5	15.3
	296.7	16.6
	302.2–302.8	23.9
	312.6–313.2	49.9
	365.0–366.3	100.0
	404.5–407.8	42.2
	435.8	77.5
	546.1	93.0
500 W xenon lamp	577.0–579.0	76.5
	303.4–304.1	18.5
	405.2–406.6	35.2
	502.3–503.1	30.3
	603.3–603.6	17.4
	704.9–705.6	12.1
	803.2–803.9	90.4
	906.2–907.1	100
999.8–1000.5	50.5	

of imidacloprid, **IPPA152001**, and **IPPA152004** during irradiation. These data were used to calculate half-lives. The irradiation experiments were not stopped until the residues of imidacloprid, **IPPA152001**, and **IPPA152004** were <1%. All tests were conducted at room temperature (25  $\pm$  3 °C). To investigate the influence of different light sources on the photodegradation kinetics, a 300 W high-pressure mercury lamp with 365 nm optical filters and a 500 W xenon lamp were also selected to irradiate the solutions of imidacloprid, **IPPA152001**, and **IPPA152004** at the concentration of  $5 \times 10^{-5}$  mol L<sup>-1</sup> under the same condition. Two hundred and fifty milliliters of **IPPA152001** and **IPPA152004** aqueous solution ( $1 \times 10^{-4}$  mol L<sup>-1</sup>) was also irradiated to observe the absorption spectrum change of **IPPA152001** and **IPPA152004** under the irradiation of the high-pressure mercury lamp. At appropriate times, depending on the photolysis rate, 10 mL of test solution was analyzed directly by UV spectrometer. One hundred milliliters of  $1 \times 10^{-3}$  mol L<sup>-1</sup> **IPPA152004** solution was irradiated under the mercury lamp, and 2 mL solutions were analyzed by LC-TOF-MS directly for characterizing photodegradation products by TOF-ESI with positive mode. LC-MS/MS was also used to confirm the structure of photo-degradation products. After irradiation of **IPPA152004** to <1%, the residue was freeze-dried and dissolved in 1 mL of methanol for GC-MS analysis.

**Light Intensity Determination.** Actinometer solutions of  $6 \times 10^{-3}$  M potassium trioxalatoferate were prepared and irradiated with the high-pressure mercury lamp (26). Dark controls were carried out at the same condition. The samples were colored by 1,10-phenanthroline in sodium acetate/sulfuric acid buffer. The colored samples were measured with a UV-vis spectrophotometer at 510 nm to provide a record of the light intensity.

**Table 2.** HPLC Gradient Conditions for Imidacloprid, IPPA152001, and IPPA152004

imidacloprid			IPPA152001			IPPA152004		
time	% buffer	%CH <sub>3</sub> CN	time	% buffer	%CH <sub>3</sub> CN	time	% buffer	%CH <sub>3</sub> CN
0	95	5	0	100	0	0	72	28
20	0	100	8	62	38	7	72	28
			12	62	38	22	0	100
			18	0	100			

**UV Measurement.** Ultraviolet spectra were measured from 200 to 500 nm with a Cary 100 Bio spectrophotometer using quartz glass cuvettes: scan rate, 600 nm min<sup>-1</sup>; average time, 0.1 s; data interval, 1.000 nm.

**HPLC Analysis Method.** The concentrations of irradiated solutions of imidacloprid, IPPA152001, and IPPA152004 were estimated by high-pressure liquid chromatography (HPLC). An Agilent 1200 series HPLC system was equipped with a Zorbax XDB-C18 column (250 mm × 4.6 mm, particle size = 5 μm), quarter pump (G1311 A), diode array detector (G1315 A), and Rheodyne injector (20 μL loop). The analyses of imidacloprid, IPPA152001, and IPPA152004 were carried out at λ<sub>max</sub> 270, 325, and 345 nm, respectively, using an acetonitrile–buffer gradient solvent system as mobile phase (Table 2), at a flow rate of 1 mL min<sup>-1</sup> and a column temperature of 25 °C. The buffer solution was prepared by adding 0.01 M ammonium acetate to distilled water and adjusting the pH value to 6 by acetic acid. The injector volume was 50 μL.

Under the conditions mentioned above, the retention time of imidacloprid was 9.875 min, that of IPPA152001 was 10.825 min, and the retention times of IPPA152004-1 and IPPA152004-2, a pair of epimers of IPPA152004, were 9.053 and 13.552 min, respectively.

**GC-MS Determinations.** GC-MS analyses were performed on an Agilent gas chromatograph model. The carrier gas was helium at a flow rate of 1.2 mL min<sup>-1</sup>. The oven temperature was programmed from 80 °C (held for 4 min) at a rate of 8 °C min<sup>-1</sup> to 260 °C, which was maintained for 5 min, then at a rate of 8 °C min<sup>-1</sup> to 300 °C, which was maintained for 17 min. The injector temperature and volume were 300 °C and 1 μL in splitless mode, respectively. Full scan and EI spectra were obtained at 70 eV for *m/z* 50–800 *u*.

**LC-TOF-ESI Analysis Method.** A liquid chromatography–time-of-flight mass spectrometry (LC-TOF-MS) system was used for structure estimation of photodegradation products. Chromatographic analysis was performed using an Agilent 1200 series HPLC system equipped with a reversed-phase Zorbax XDB-C18 analytical column (4.6 mm × 150 mm × 5 μm particle size). Solvent A was water with 0.015% formic acid, and solvent B was acetonitrile. The flow rate was 0.5 mL min<sup>-1</sup> with column temperature at 30 °C, and the injection volume was 20 μL. The gradient elution conditions were initially A (100%), holding 100% A for 10 min, programming to 20% B over 30 min, holding 20% B for 10 min, programming to 60% B over 20 min, then programming to 100% B over 20 min. The total analysis time was 90 min. This HPLC system was connected to a TOF mass spectrometer (Agilent Technologies 6210) equipped with an electrospray interface. The analysis mode of ionization was electrospray ionization (ESI, positive). The operation conditions were as follows: capillary, 3000 V; nebulizer, 50 psi; drying gas, 6 L min<sup>-1</sup>; gas temperature, 350 °C; skimmer voltage, 60 V; fragmentor voltage, 250 V. The scanned *m/z* range was 50–400 Da. The data were recorded and analyzed with Agilent MassHunter Workstation Software Qualitative Analysis version B.01.03.

**LC-MS/MS Analysis Method.** LC-MS/MS was used for structure estimation of photodegradation products. Chromatographic analysis was performed using a Waters Acquity UPLC system equipped with a reversed-phase Waters XTerra MS C18 HPLC analytical column (4.6 mm × 150 mm × 5 μm particle size). Solvent A was water with 0.1% formic acid, and solvent B was acetonitrile. The flow rate was 0.2 mL min<sup>-1</sup> with column temperature at 25 °C, and the injection volume was 5 μL. The gradient elution conditions were initially A (80%), holding 80% A for 20 min, programming to 100% B over 3 min, holding 100% B for 4 min. The total analysis time was 27 min. This HPLC system was connected to an ESCI mass spectrometer (Micromass Quattro Micro API LC/MS/MS instrument). The analysis mode of ionization was electrospray ionization (ESI, positive). The operation conditions were as follows: capillary, 3000 V; collision energy, 25 V; cone, 20 V; drying gas, 6 L min<sup>-1</sup>; gas temperature, 350 °C. The scanned *m/z* range was 50–500 Da.

**Synthesized Standard Compounds.** 1-((6-Chloropyridin-3-yl)methyl)-8-nitro-1,2,3,5,6,7-hexahydroimidazo[1,2-*a*]pyridin-5-ol (IPPA152001) (25): mp 170.6–171.1 °C; <sup>1</sup>H NMR (400 Mz, DMSO-*d*<sub>6</sub>) δ 8.34 (d, *J* = 2.1 Hz, 1H), 7.80 (dd, *J*<sub>1</sub> = 2.4 Hz, *J*<sub>2</sub> = 8.2 Hz, 1H), 7.49 (d, *J* = 8.2 Hz, 1H), 6.29 (d, *J* = 6.2 Hz, 1H), 4.82 (m, 1H), 4.73 (d, *J* = 15.5 Hz, 1H), 4.59 (d, *J* = 15.5 Hz, 1H), 3.58–3.74 (m, 4H), 3.11–3.16 (m, 1H), 1.88–1.95 (m, 1H), 1.69–1.75 (m, 1H), 1.03 (d, *J* = 6.6 Hz, 1H); <sup>13</sup>C NMR (100 Mz, DMSO-*d*<sub>6</sub>) δ 158.5, 149.6, 139.7, 132.6, 74.4, 109.3, 76.0, 51.9, 49.8, 45.2, 38.6, 28.3, 20.1. HRMS (EI+): calcd for C<sub>14</sub>H<sub>17</sub>N<sub>4</sub>O<sub>3</sub><sup>35</sup>Cl (M<sup>+</sup>), 324.0989; found, 324.1014; calcd for C<sub>14</sub>H<sub>17</sub>N<sub>4</sub>O<sub>3</sub><sup>37</sup>Cl (M<sup>+</sup>), 326.0960; found, 326.0964. Anal. Calcd for C<sub>14</sub>H<sub>17</sub>ClN<sub>4</sub>O<sub>3</sub>: C, 51.78; H, 5.28; N, 17.25. Found: C, 51.91; H, 5.15; N, 16.95.

1-((6-Chloropyridin-3-yl)methyl)-7-methyl-8-nitro-5-propoxy-1,2,3,5,6,7-hexahydroimidazo[1,2-*a*]pyridine (IPPA152004) (25): mp 130.2–131.9 °C; <sup>1</sup>H NMR (400 MHz, CDCl<sub>3</sub>) δ 8.31–8.33 (m, 1H), 7.86 (dd, *J*<sub>1</sub> = 2.4 Hz, *J*<sub>2</sub> = 8.4 Hz, 0.5H), 7.82 (dd, *J*<sub>1</sub> = 2.4 Hz, *J*<sub>2</sub> = 8.2 Hz, 0.5H), 7.33 (dd, *J*<sub>1</sub> = 0.8 Hz, *J*<sub>2</sub> = 1.2 Hz, 0.5H), 7.31 (dd, *J*<sub>1</sub> = 0.8 Hz, *J*<sub>2</sub> = 1.2 Hz, 0.5H), 4.88 (d, *J* = 15.2 Hz, 0.5H), 4.82 (d, *J* = 15.2 Hz, 0.5H), 4.61–4.67 (m, 1H), 4.55 (dd, *J*<sub>1</sub> = 3.6 Hz, *J*<sub>2</sub> = 6.0 Hz, 0.5H), 4.50 (t, *J* = 3.6 Hz, 0.5H), 3.95–4.02 (m, 0.5H), 3.81–3.86 (m, 0.5H), 3.64–3.72 (m, 1H), 3.35–3.59 (m, 5H), 2.14–2.21 (m, 0.5H), 1.99–2.01 (m, 1H), 1.75–1.82 (m, 0.5H), 1.54–1.65 (m, 2H), 1.22–1.27 (d, *J* = 6.8 Hz, 0.5H), 1.23 (d, *J* = 6.8 Hz, 0.5H), 0.95 (t, *J* = 6.2 Hz, 0.5H), 0.92 (t, *J* = 6.2 Hz, 0.5H). HRMS (EI+) calcd for C<sub>17</sub>H<sub>23</sub>N<sub>4</sub>O<sub>3</sub><sup>35</sup>Cl (M<sup>+</sup>), 366.1459; found, 366.1487.

## RESULTS AND DISCUSSION

### Photodegradation of Imidacloprid, IPPA152001, and IPPA152004.

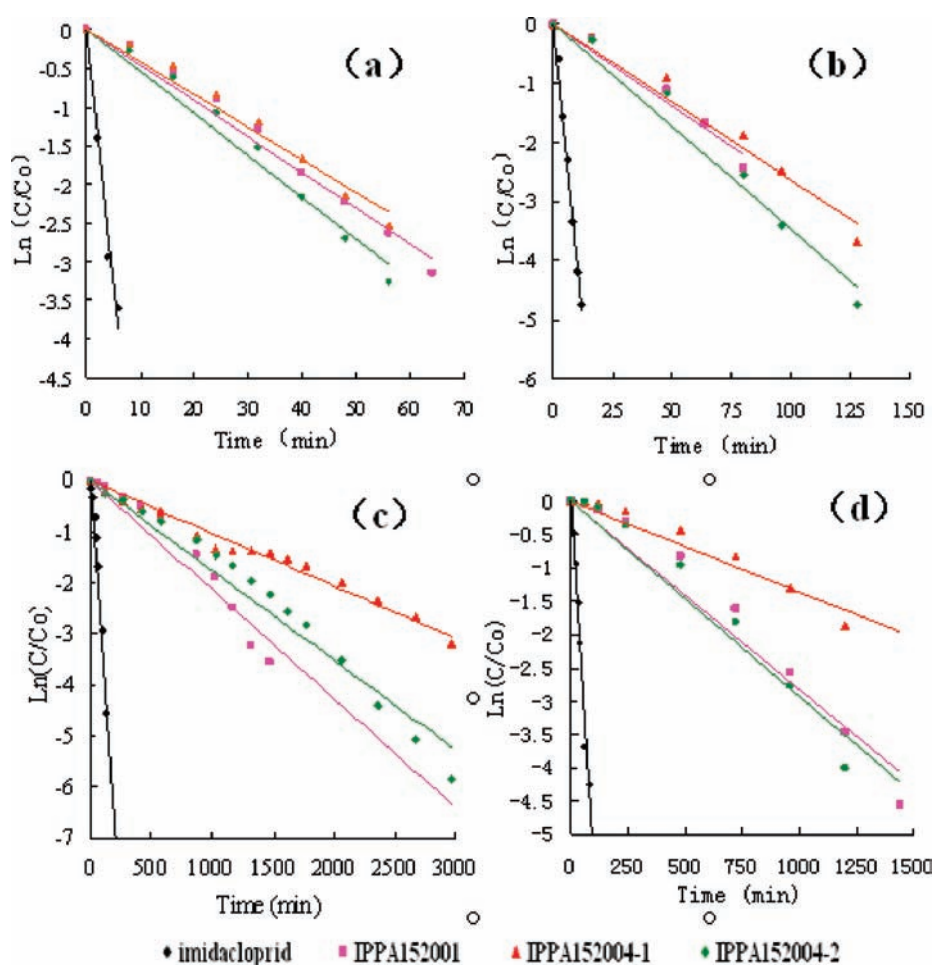
The photodegradation kinetics of imidacloprid, IPPA152001, and IPPA152004 were calculated by the residues of peak area versus irradiation time. The relative concentrations of imidacloprid, IPPA152001 and IPPA152004 were plotted as ln(*C/C*<sub>0</sub>) versus irradiation time, where *C* and *C*<sub>0</sub> were the concentrations of irradiated solutions at time *t* and *t* = 0. The linear response (*R*<sup>2</sup>) indicated that the photodegradation followed pseudo-first-order kinetics, which could be described by the eq 1. The degradation rate constant (*k*) was calculated from the slope of the line of ln(*C/C*<sub>0</sub>) versus irradiation time.

$$\ln(C/C_0) = -kt \quad (1)$$

The data of photodegradation rate constants (*k*), half-lives (*t*<sub>1/2</sub>), and linear response (*R*<sup>2</sup>) for imidacloprid, IPPA152001, and IPPA152004 are shown in Table 3. The initial concentration increased from 1 × 10<sup>-5</sup> to 5 × 10<sup>-5</sup> mol L<sup>-1</sup> when a 300 W high-pressure mercury lamp was used as light source. The results indicated that the lower the initial concentration of the solution, the faster the photolysis rate. At an initial concentration of 5 × 10<sup>-5</sup> mol L<sup>-1</sup>, imidacloprid disappeared totally after 1 h of irradiation, whereas 18.8% of IPPA152001, 20.6% of IPPA152004-1, and 12% of IPPA152004-2 were kept. The results showed that the degradation process strongly depended on the chemical structure and the initial concentration of substrates, which may be due to the competition between parent compounds and their photodegradation products for limited photons (13). IPPA152004-1 and IPPA152004-2 were two epimers of IPPA152004. In the conformation of IPPA152004-1, the methyl and propoxyl group pointed to the opposite orientation at the retention time of 9.053 min, and the two groups of IPPA152004-2 locate in the same side of the tetrahydropyridine ring at the retention time of 13.552 min. The conformation was presumed on the basis of our previous research (25). The ratio IPPA152004-1 and IPPA152004-2 is 1:1 based on the analysis of HPLC (which is available in the Supporting Information). The epimer IPPA152004-1 was more stable than the other, which implies that the photodegradation rate had a close relationship with the space structure of the compounds. In a word, it was obvious that the stability of the compounds with the motif of the tetrahydropyridine ring was better than that of imidacloprid.

**Table 3.** Photodegradation Rate Constants ( $k$ ), Half-Lives ( $t_{1/2}$ ), and Linear Responses ( $R^2$ ) for Imidacloprid, IPPA152001, and IPPA152004 at Various Initial Concentrations under the Irradiation of a 300 W High-Pressure Mercury Lamp with or without a 365 nm Optical Filter and a 500 W Xenon Lamp

light source	sample	concentration (mol/L)	$k$	$t_{1/2}$ (min)	$R^2$
300 W high-pressure mercury lamp	imidacloprid	$1 \times 10^{-5}$	0.6443	1.08	0.9732
		$5 \times 10^{-5}$	0.4029	1.72	0.9944
	IPPA152001	$1 \times 10^{-5}$	0.0422	16.43	0.9719
		$5 \times 10^{-5}$	0.0275	25.21	0.9619
	IPPA152004-1	$1 \times 10^{-5}$	0.0462	15.00	0.9810
		$5 \times 10^{-5}$	0.0263	26.36	0.9686
500 W xenon lamp	IPPA152004-2	$1 \times 10^{-5}$	0.0543	12.77	0.9749
		$5 \times 10^{-5}$	0.0347	19.98	0.9714
	imidacloprid	$5 \times 10^{-5}$	0.0337	20.6	0.9619
	IPPA152001	$5 \times 10^{-5}$	0.0021	330.1	0.941
300 W high-pressure mercury lamp with a 365 nm optical filter	IPPA152004-1	$5 \times 10^{-5}$	0.001	693.1	0.9773
		$5 \times 10^{-5}$	0.0018	385.1	0.9673
	imidacloprid	$5 \times 10^{-5}$	0.055	12.6	0.9856
	IPPA152001	$5 \times 10^{-5}$	0.0028	247.6	0.9588
300 W high-pressure mercury lamp with a 365 nm optical filter	IPPA152004-1	$5 \times 10^{-5}$	0.0014	495.1	0.9472
		$5 \times 10^{-5}$	0.0029	239.0	0.9515
	imidacloprid	$5 \times 10^{-5}$	0.055	12.6	0.9856
	IPPA152001	$5 \times 10^{-5}$	0.0028	247.6	0.9588

**Figure 1.** Photodegradation curve of imidacloprid, IPPA152001, and IPPA152004 irradiated with different light sources: (a) imidacloprid, IPPA152001, and IPPA152004 of  $1 \times 10^{-5}$  mol/L irradiated with a 300 W high-pressure mercury lamp; (b) imidacloprid, IPPA152001, and IPPA152004 of  $5 \times 10^{-5}$  mol/L irradiated with a 300 W high-pressure mercury lamp; (c) imidacloprid, IPPA152001, and IPPA152004 of  $5 \times 10^{-5}$  mol/L irradiated with a 500 W xenon lamp; (d) imidacloprid, IPPA152001, and IPPA152004 of  $5 \times 10^{-5}$  mol/L irradiated with a 300 W high-pressure mercury lamp with a 365 nm optical filter.

The effect of different light sources was investigated as shown in Figure 1. Obviously, photodegradation kinetics strongly relied on lamp energy output at the same concentration. The degradation rates of imidacloprid, IPPA152001, and IPPA152004 with

different light resources followed the order of 300 W high-pressure mercury lamp (Figure 1b) > 300 W high-pressure mercury lamp with 365 nm optical filter (Figure 1d) > 500 W xenon lamp (Figure 1c). As listed in Figure 1, the rate of

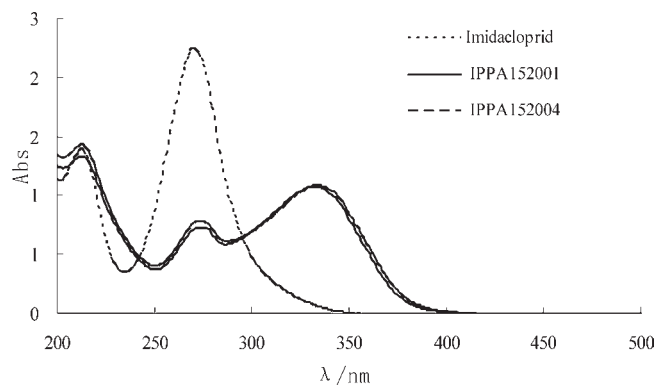


**Figure 2.** Ultraviolet absorption of imidacloprid, IPPA152001, and IPPA152004.

degradation was according to the order imidacloprid > IPPA152001 ≥ IPPA152004. It was concluded that the stability of neonicotinoid compounds with *cis*-nitro configuration increased dramatically due to introduction of the tetrahydropyridine ring.

**Quantum Yield Calculations.** Using potassium trioxalatoferate as chemical actinometer, quantum yields of photodegradation were calculated by dividing the amount of degradation by the number of adsorbed photons at zero time of irradiation following the equations below (27):

$$I_{(0,\lambda)} = k_0/\Phi_{(b,\lambda)} \quad (2)$$

$$I_{(abs,\lambda)} = I_{(0,\lambda)}(1 - 10^{-A(\lambda)}) \quad (3)$$

$$\Phi(\lambda) = [dn/dt]/I_{(0,\lambda)}(1 - 10^{-A(\lambda)}) \quad (4)$$

$I_{(0,\lambda)}$  was the light intensity of the high-pressure mercury lamp at wavelength  $\lambda$ ;  $I_{(abs,\lambda)}$  was the absorbed light intensity of IPPA152001 and IPPA152004 with irradiation by the mercury lamp;  $k_0$  was the degradation rate of potassium trioxalatoferate;  $\Phi_{(b,\lambda)}$  was the calculated quantum yield of ferrous ion with the irradiation of mercury lamp at wavelength  $\lambda$ ;  $\Phi(\lambda)$  was the calculated quantum yield of IPPA152001 and IPPA152004 with irradiation by the mercury lamp at wavelength  $\lambda$ ;  $A(\lambda)$  was the absorbance of samples. By chemical actinometer determination, the degradation rate of potassium trioxalatoferate was  $6 \times 10^{-6} \text{ s}^{-1}$ ; the quantum yield of ferrous ion with the irradiation of mercury lamp at wavelength 365 nm was 1.21 by the manuals of photochemistry (28). Therefore, the light intensity of the high-pressure mercury lamp at wavelength 365 nm was  $4.96 \times 10^{-6} \text{ mol L}^{-1} \text{ s}^{-1}$ . According to the equation above, the quantum yield of IPPA152001 was calculated as  $5.16 \times 10^{-4} \text{ mol einstein}^{-1}$  at 365 nm and the quantum yields of IPPA152004-1 and IPPA152004-2 were  $3.73 \times 10^{-4}$  and  $4.93 \times 10^{-4} \text{ mol einstein}^{-1}$ , respectively.

**UV Spectral Analysis.** The UV spectrum of imidacloprid in aqueous solution (Figure 2) showed that the maximum absorption wavelength of imidacloprid was 270 nm, whereas the maximum absorption wavelengths of IPPA152001 and IPPA152004 were around 330 nm because of the introduction of the tetrahydropyridine ring. All of the UV spectra exhibited similar features.

The absorption peaks near 210 nm of imidacloprid, IPPA152001, and IPPA152004 were observed due to the  $\pi-\pi^*$  system of pyridine, and the band at 270 nm indicated the absorption of delocalized diene system conjugated with amidine, double bond, and nitro group of imidacloprid (29). Due to the introduction of

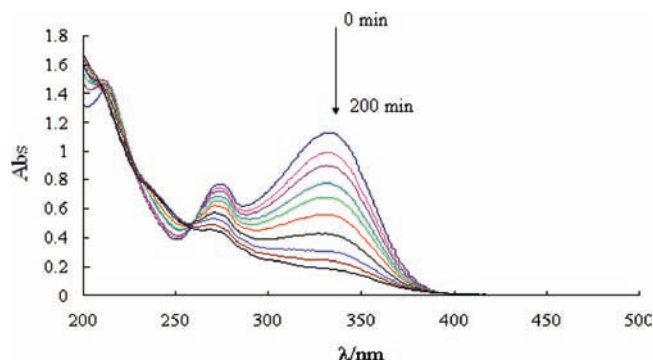


**Figure 3.** Ultraviolet absorption of IPPA152001 after different times of photodegradation (0–200 min).

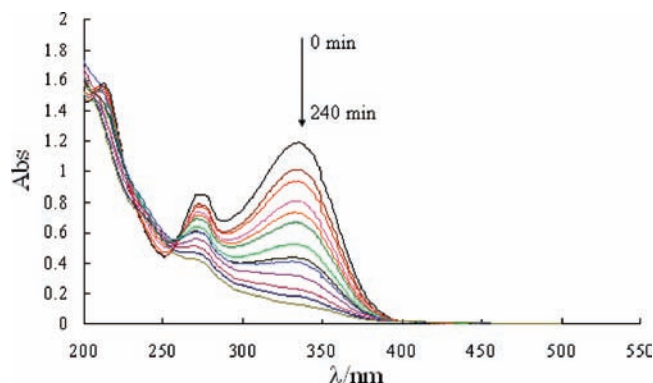


**Figure 4.** Ultraviolet absorption of IPPA152004 after different times of photodegradation (0–220 min).

the tetrahydropyridine ring, the maximum absorption wavelengths of IPPA152001 and IPPA152004 red-shifted from 270 to 330 nm (30). The change of UV spectra of IPPA152001 and IPPA152004 during the photolysis process under mercury lamp irradiation is shown in Figures 3 and 4. The absorption intensities of IPPA152001 and IPPA152004 at 270 and 330 nm decreased with irradiation time, which suggested that the conjugation system consisting of amidine, a nitro group, and the tetrahydropyridine ring was destroyed rapidly.

**Photodegradation Products and Pathway.** The major photodegradation products of IPPA152004 had been analyzed by a combination of gas chromatography–mass spectrometry (GC-MS), high-performance liquid chromatography–time-of-flight mass spectrometry (LC-MS) with ESI positive mode, and LC-MS/MS. In this study, 22 degradation products were put forward by LC-TOF-ESI spectra; the measured and calculated masses of the protonated ions, the error between them, and the proposed empirical formulas are shown in Table 4. Eleven compounds were also characterized by GC-MS on the basis of combined library mass spectra.

The possible photodegradation pathway in aqueous solution under mercury lamp irradiation was proposed. The photochemical transformation of IPPA152004 underwent three pathways, which were presented by the change of parent compound IPPA152004 (Figure 7): (i) conversion of nitro to nitroso (the main pathway); (ii) removal of propyl; (iii) introduction of hydroxyl group to tetrahydropyridine.

At first, the nitro group of the parent compound lost one oxygen and formed **1a**, then **1a** lost a nitroso and became compound **1c** shown in HPLC. Two groups of peaks of **1c** were observed, and their retention times were 45.332, 46.261, 47.639, and 48.319 min, respectively, and the integration of all the peaks

**Table 4.** LC-ESI Retention Times ( $t_R$ ), and Spectral Characteristics of **IPPA152004** Photoproducts

no.	$t_R$ (min)	formula	mass, calcd	mass	difference (ppm)	daughter ions (relative abundance)
<b>IPPA152004</b>	52.899	$C_{17}H_{23}ClN_4O_3$	366.14788	366.14587	-5.5	367.15516 ([M + H], 100), 369.15347 (29.7), 368.1576 (16.0), 370.1559 (5.0)
<b>IPPA152004</b>	60.283	$C_{17}H_{23}ClN_4O_3$	366.14708	366.14587	-3.32	367.15437 ([M + H], 8.4), 389.13719 ([M + Na], 11.3), 350.15216 (6.5), 306.13875 (100), 308.13578 (33.2), 137.10791 (40.1)
<b>1a</b>	47.257	$C_{17}H_{23}ClN_4O_2$	350.15158	350.15095	-1.8	351.15886 ([M + H], 100), 353.15629 (30.0), 320.15263 (17.4), 322.1502 (5.1)
<b>1a</b>	59.105	$C_{17}H_{23}ClN_4O_2$	350.15113	350.15095	-0.51	351.1584 ([M + H], 100), 353.15629 (30.4), 153.10179 (6.8)
<b>1b</b>	51.389	$C_{17}H_{24}ClN_3O$	321.15964	321.16079	3.57	322.16878 ([M + H], 100), 324.16721 (29.2)
<b>1b</b>	58.607	$C_{17}H_{24}ClN_3O$	321.12558	321.1244	-3.67	322.13286 ([M + H], 100), 324.13038 (32.5)
<b>1c</b>	45.332	$C_{17}H_{24}ClN_3O_2$	337.15716	337.1557	-4.33	338.1651 ([M + H], 100), 340.1625 (35.94626), 278.1069 (39.98821), 280.1040 (12.08925), 126.0110 (7.368172)
<b>1c</b>	46.261	$C_{17}H_{24}ClN_3O_2$	337.15665	337.1557	-2.37	338.16379 ([M + H], 100), 340.16101 (35.0), 278.10559 (39.6), 280.10419 (10.6), 126.01034 (6.9)
<b>1c</b>	47.639	$C_{17}H_{24}ClN_3O_2$	337.15837	337.1557	-7.92	338.16427 ([M + H], 100), 340.16108 (40.4), 278.10549 (34.7), 280.10303 (10.4)
<b>1c</b>	48.319	$C_{17}H_{24}ClN_3O_2$	337.15734	337.1557	-4.86	338.16403 ([M + H], 69.5), 340.16112 (29.7), 320.15308 (5.9), 278.10585 (100), 280.10321 (31.8), 126.01038 (8.2)
<b>1d</b>	30.646	$C_{11}H_{20}N_2O_2$	212.15359	212.15248	-5.26	213.16088 ([M + H], 100), 153.10254 (26.2)
<b>1d</b>	33.783	$C_{11}H_{20}N_2O_2$	212.15387	212.15248	-6.58	213.16148 ([M + H], 31.9), 153.10366 (100), 108.04546 (15.0)
<b>1d</b>	34.579	$C_{11}H_{20}N_2O_2$	212.15383	212.15248	-6.39	213.16099 ([M + H], 71.6), 153.10309 (100), 125.10804 (7.2), 108.04516 (18.5)
<b>1d</b>	35.874	$C_{11}H_{20}N_2O_2$	212.15357	212.15248	-5.16	213.16086 ([M + H], 31.3), 153.1031 (100), 108.0451 (13.6)
<b>2a</b>	24.806	$C_{14}H_{17}ClN_4O_3$	324.09963	324.09892	-2.21	325.10701 ([M + H], 64.4), 327.10496 (19.4), 170.08145 (100), 172 (35.8), 142.08621 (83.8), 144.08712 (24.1), 126.01075 (20.0)
<b>2b</b>	28.025	$C_{14}H_{17}ClN_4O_2$	308.10595	308.104	-6.33	309.11323 ([M + H], 100), 311.11163 (30.8), 183.10111 (25.2), 185.11231 (7.9), 166.09726 (9.1)
<b>2b</b>	32.472	$C_{14}H_{17}ClN_4O_2$	308.10482	308.104	-2.66	309.1121 ([M + H], 100), 311.11011 (37.0), 277.09075 (8.0), 210.04458 (17.8)
<b>2c</b>	30.481	$C_{14}H_{16}ClN_3O$	279.11415	279.11384	-1.12	280.12143 ([M + H], 100), 282.11942 (31.9), 213.16007 (25.8), 215.16221 (7.8), 195.1497 (6.3), 154.08973 (7.5)
<b>2d</b>	27.427	$C_{14}H_{16}ClN_3O_2$	295.11035	295.10875	-5.42	296.11763 ([M + H], 100), 298.11488 (33.9), 126.01105 (22.3), 128.00857 (6.2)
<b>2d</b>	28.191	$C_{14}H_{16}ClN_3O_2$	295.10973	295.10875	-3.32	296.11701 ([M + H], 100), 298.1141 (31.1), 126.01076 (27.5), 128.00819 (7.6)
<b>2e</b>	59.669	$C_{14}H_{16}ClN_3O_2$	293.09328	293.0931	0.61	294.10056 ([M + H], 37.2), 296.10106 (9.4), 279.11254 (24.0), 281.11321 (8.2), 153.10221 (100), 155.12332 (35.8), 135.09144 (17.0)
<b>2f</b>	41.183	$C_9H_{10}ClN_3$	195.05636	195.05633	-0.2	196.06364 ([M + H], 100), 198.06085 (32.8), 126.01063 (93.0), 128.00818 (29.9), 98.99897 (5.7)
<b>2h</b>	14.368	$C_8H_8ClN_3$	181.04143	181.04067	-4.19	182.04846 ([M + H], 100), 184.04576 (27.3), 139.00549 (44.4), 141.00638 (12.4)
<b>2i</b>	20.873	$C_8H_6ClN_3$	179.02489	179.02502	0.73	180.03217 ([M + H], 100), 182.03052 (36.0), 139.00073 (32.6), 141.00084 (10.1), 91.0502 (5.9)
<b>2k</b>	6.785	$C_8H_{14}N_2O$	154.11063	154.11061	-0.13	155.11791 ([M + H], 100), 139.06074 (7.7), 111.09144 (60.4), 85.07543 (39.6)
<b>2m</b>	8.013	$C_8H_{14}N_2O_2$	170.10651	170.10553	-5.8	171.11379 ([M + H], 100), 108.04623 (7.6)
<b>2m</b>	12.145	$C_8H_{14}N_2O_2$	170.1064	170.10553	-5.15	171.11368 ([M + H], 100), 153.10286 (8.1), 108.04497 (11.3)
<b>2m</b>	13.539	$C_8H_{14}N_2O_2$	170.10637	170.10553	-4.97	171.11365 ([M + H], 100), 153.10246 (12.9), 108.04505 (19.1)
<b>2n</b>	32.289	$C_8H_{12}N_2O$	152.09591	152.09496	-6.25	153.10319 ([M + H], 100), 125.10809 (11.4)
<b>3a</b>	47.983	$C_{17}H_{23}ClN_4O_4$	382.14238	382.14078	-4.19	383.14966 (100), 385.14823 (34.0), 340.5675 (9.6), 308.11991 (51.0), 310.11982 (16.3), 183.07643 (16.4)
<b>3a</b>	55.222	$C_{17}H_{23}ClN_4O_4$	382.14037	382.14078	1.07	383.14765 (78.9), 385.14676 (27.7), 308.11892 (40.6), 310.11873 (12.5), 294.1005 (100), 296.1008 (36.1), 169.05701 (29.0), 171.05782 (9.5)
<b>3b</b>	41.797	$C_{17}H_{21}ClN_4O_3$	364.13159	364.13022	-3.78	365.13887 ([M + H], 36.2), 367.1421 (16.5), 319.1448 (15.4), 289.13321 (43.5), 291.13423 (13.2), 16.12313 (100), 165.12545 (35.7)
<b>3c</b>	48.319	$C_{17}H_{22}ClN_3O$	319.14636	319.14514	-3.83	320.1536 ([M + H], 13.6), 322.15042 (5.3), 276.09094 (100), 278.08974 (36.2), 248.09544 (17.2), 223.05204 (28.6), 225.06211 (9.1)
<b>3d</b>	35.708	$C_{14}H_{16}ClN_3O$	277.09902	277.09819	-3.01	278.10626 ([M + H], 100), 280.09081 (14.1)
<b>3d</b>	36.803	$C_{14}H_{16}ClN_3O$	277.09769	277.09819	1.79	278.10523 ([M + H], 8.6), 280.1043 (2.7), 264.09108 (100), 266.08845 (30.5)

of **1c** in the high-performance liquid chromatogram at 254 nm was about 23.53%. The variation of **1c** abundance in the photolysis process of **IPPA152004** under mercury lamp irradiation is shown in **Figure 5**. After 12 h of irradiation, the amount of product **1c** reached the largest value. For accurate mass measurement of this product, only the empirical formula  $C_{17}H_{24}ClN_3O_2$  was reasonable, and the error was also low enough for the identification. To further confirm the structure of **1c**, LC-MS/MS analysis was also carried out; the main daughter ions of **1c** were obtained, which clearly confirmed the position of C=O in the structure of **1c**. The mass spectra of **1c** and its product ions are available in the Supporting Information, and the progress of splitting is described in **Figure 6**.

Furthermore, the obvious daughter ion at  $m/z$  278.1055 was formed by the loss of propoxyl group from the parent compound. Compared with the parent compound (**IPPA152004**), protonated ion with  $m/z$  351.15886 was attributed to loss of oxygen, whereas the empirical formula was calculated as  $C_{17}H_{23}ClN_4O_2$ , and the structure is shown in **Figure 7 (1a)**. The retention times were

47.257 and 59.105 min. It was presumed that the nitro group of **IPPA152004** converted to nitroso, which was similar to the reported photodegradation of imidacloprid (**13**, **17**).

Obviously, the  $m/z$  of protonated ion of product **2a** was the same as **IPPA152001**, which could be generated by the loss of propoxyl group from parent compound **IPPA152004**. It was confirmed by the retention time in their HPLC spectrum. The nitroso produced in the degradation process was also presumed from **2a** to **2b** just like the case above, which was from the parent compound to **1a**. The ion  $m/z$  was 309.1132 and 325.1070, respectively, which demonstrated obviously a loss of oxygen. The compounds with nitroso (**1a**, **2b**) were so unstable that an elimination reaction occurred and formed products **1b** and **2c** with  $m/z$  322.1687 and 280.1214 (**13**, **17**).

In addition, during the photolysis reaction process, free radical  $\cdot OH$  usually was obtained from  $H_2O$  and might attack the tetrahydropyridine ring of **IPPA152004**, forming the product **3a** with a mass-to-charge ratio of 383.1496. Products **3b** and **2l** were formed via elimination of  $H_2O$  from the dihydropyridine ring of

compounds **3a** and **2k**, which were speculated according to accurate mass measurement of **3b** and fragment of **2l** in the GC-MS spectra. The photodegradation products **1b**, **2c**, **3d**, **2f**, **2k**, and **2n** with C=C double bond were oxidized directly to generate products **1c**, **2d**, **2e**, **2j**, **2m**, and **2p**, respectively, whereas **2d** and **2m** could be further oxidized to form **2e** and **2p**. The degradation products **1d** and **2k** formed by the cleavage of C–N between chloropyridine and imidazolidine were also detected by LC-MS. Finally, by GC-MS analysis, the conversion of **2j** to **2u** was in accordance with the photodegradation of imidacloprid, which had been reported (8, 9, 11, 13, 14, 17). The proposed products are listed in Table 5 and Figure 7. During these three processes, it was also found that the same degradation products were obtained by different process; for example, **2d** could be obtained from path 1 and 2 and **2e** from path 2 and 3. This means the degradation process is very complicated and needs to be clearly elucidated in further research.

By comparison of the products of GC-MS and LC-MS, it was found that the molecular weights of compounds were less than 211 in GC-MS spectrum. The reason might be that the chemicals with the motif of 1-((6-chloropyridin-3-yl)methyl)octahydroimidazo[1,2-*a*]pyridine could not be detected in GC-MS. In addition, it was obviously observed that all of the compounds identified in GC-MS could not be detected in the experiment of LC-MS, except 7-methyl-2,3,6,7-tetrahydroimidazo[1,2-*a*]pyridine-5(1*H*)-one (**2n**). It was easy to understand as the amount

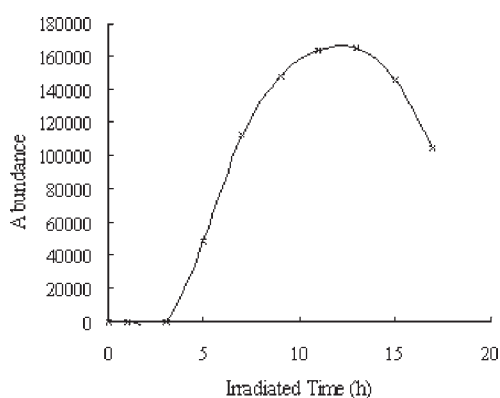


**Figure 5.** Amount of photoproduct 1-((6-chloropyridin-3-yl)methyl)-7-methyl-5-propoxyhexahydroimidazo[1,2-*a*]pyridin-8(5*H*)-one (**1c**) formed during IPPA152004 photodegradation with the concentration of  $1 \times 10^{-3}$  mol L<sup>-1</sup> irradiated with a 300 W high-pressure mercury lamp.

of degradation products of IPPA152004 in GC-MS analysis was 500 times than that of LC-MS.

On the basis of the analysis of photodegradation products of IPPA152004, a distinct photolysis pathway is

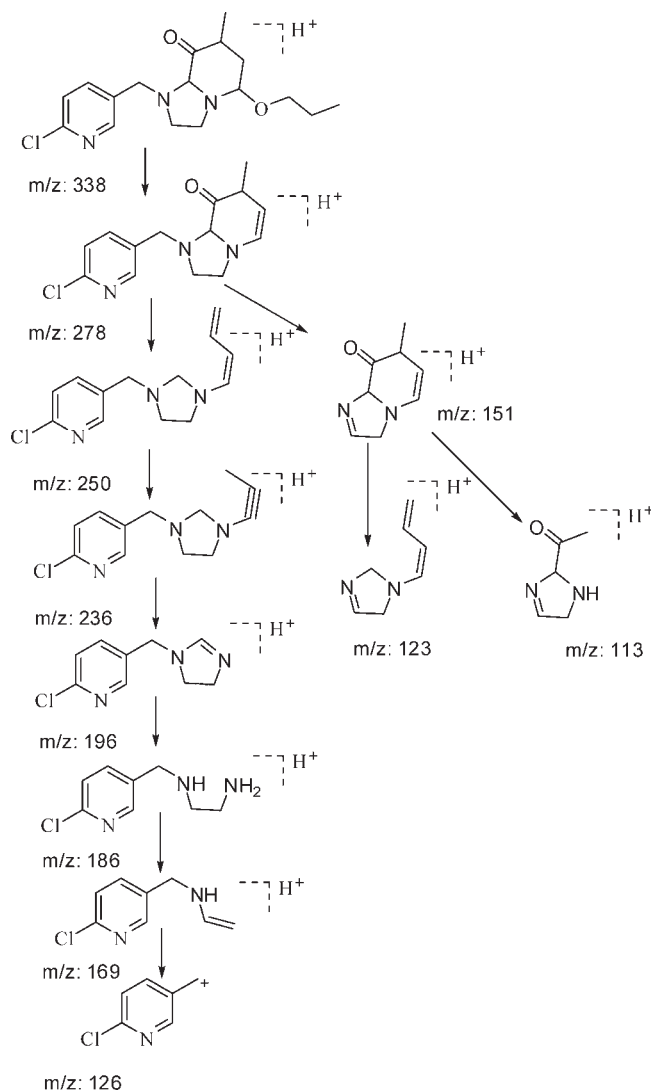


**Figure 6.** Proposed daughter ions and clearance pathways for **1c** by LC-MS/MS.

**Table 5.** GC-MS Retention Times ( $t_R$ ) and Mass Spectral Data of Photoproducts of IPPA152004

code	$t_R$ (min)	compound name	GC-MS fragment [ $m/z$ (relative abundance)]
<b>2g</b>	19.430	5-((1 <i>H</i> -imidazol-1-yl)methyl)-2-chloro-pyridine	193 (36.9), 195 (13.6), 126 (100), 128 (34.2), 99 (13.1), 90 (15.6)
<b>2i</b>	19.925	2-chloro-1,6-naphthyridin-8-amine	179 (100), 181 (34.3), 144 (62.2), 146 (21.6), 126 (35.4), 128 (11.2)
<b>2l</b>	9.582	7-methyl-1,2,3,7-tetrahydroimidazo[1,2- <i>a</i> ]pyridine	168 (34.6), 99 (100)
<b>2p</b>	17.501	7-methylhexahydroimidazo[1,2- <i>a</i> ]pyridine-5,8-dione	140 (100), 112 (43.5), 103 (13.0), 85 (10.0), 76 (20.1), 51 (17.1)
<b>2q</b>	8.592	<i>N</i> -((6-chloropyridin-3-yl)methyl)formamide	170 (75.4), 172 (28.2), 150 (48.1), 152 (14.2), 141 (100), 143 (31.5), 126 (33.3), 128 (10.2), 114 (29.6), 78 (33.3), 80 (10.1)
<b>2r</b>	15.588	6-chloronicotinamide	156 (68.9), 158 (26.4), 140 (100), 142 (35.2), 112 (42.6), 114 (12.6), 76 (21.3)
<b>2s</b>	8.268	6-chloronicotinonitrile	140 (100), 142 (38.1), 112 (47.8), 114 (15.7), 76 (19.6)
<b>2t</b>	8.265	6-chloronicotinaldehyde	140 (100), 142 (17.6), 112 (43.5), 114 (12.9), 103 (13.0), 85 (10.0), 76 (20.1), 51 (17.1)
<b>2u</b>	10.832	methyl 6-chloronicotinate	171 (26.9), 173 (9.6), 140 (100), 142 (35.2), 112 (42.4), 114 (13.1), 85 (13.8), 76 (16.7)
<b>2w</b>	10.546	2-chloro-5-(chloromethyl)pyridine	161 (25.1), 163 (9.2), 126 (100), 128 (35.7), 99 (13.6), 90 (16.5), 63 (13.6)
<b>2j</b>	22.609	1-((6-chloropyridin-3-yl)methyl)-imidazolidin-2-one	211 (100), 213 (36.2), 182 (16.1), 140 (28.2), 126 (56.4), 128 (16.8), 99 (41.9), 101 (13.2)

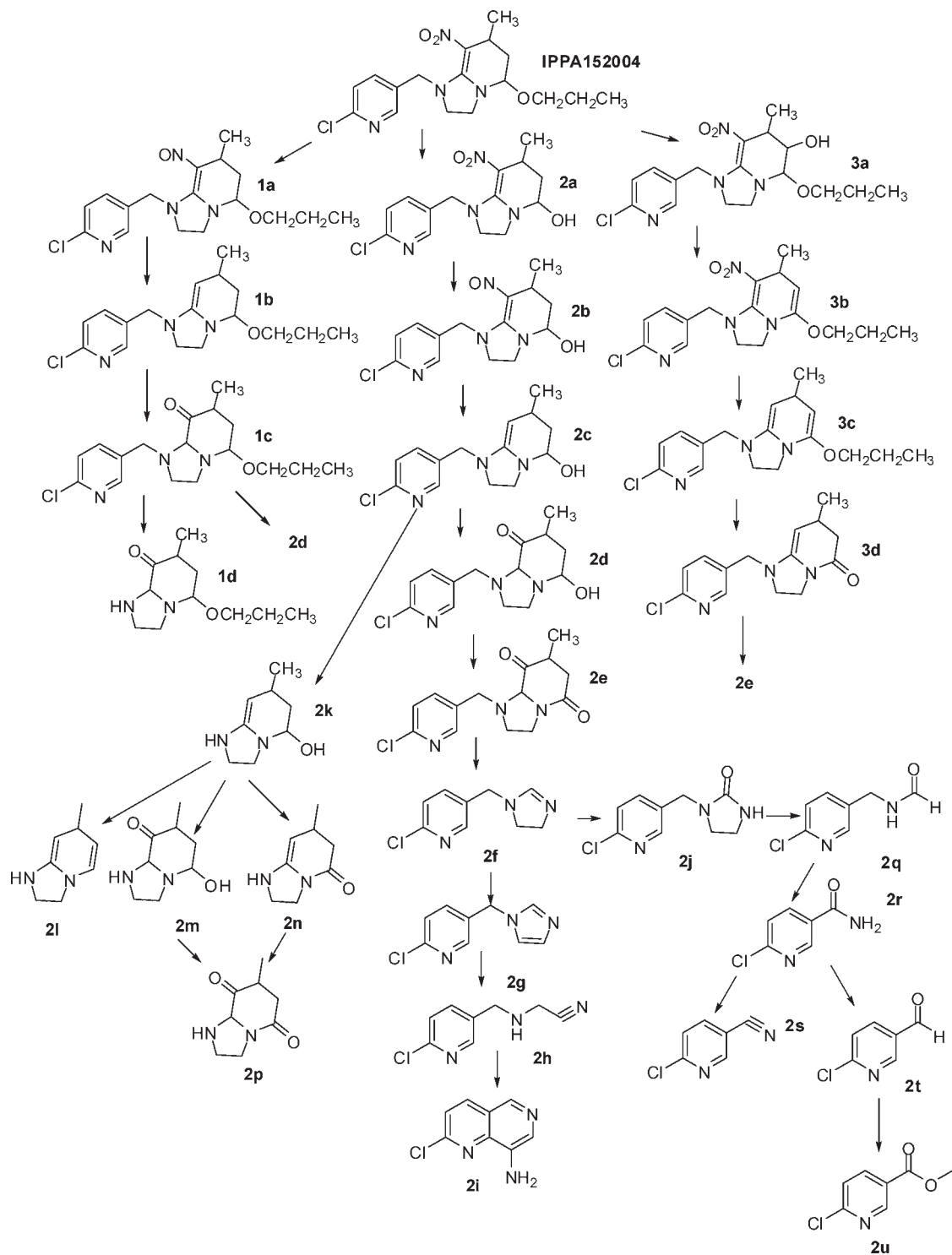


**Figure 7.** Hypothetical photodegradation pathway of **IPPA152004** by photolysis.

shown in **Figure 7**. The photodegradation of **IPPA152004** mainly occurred on the tetrahydropyridine ring rather than on the imidazolidine ring, including the elimination of nitro and photooxidation as shown in **Figure 7**. However, in the normal degradation pathway of imidacloprid, cleavage of the imidazolidine ring was usually detected. Moreover, the degradation products of imidacloprid were strikingly different from their parent compound, but most degradation products of **IPPA152004** had a scaffold similar to that of the tetrahydropyridine ring. This result was in accordance with the analysis of UV spectra.

In conclusion, photodegradation of novel nitromethylene neonicotinoids with tetrahydropyridine-fixed *cis* configuration **IPPA152001** and **IPPA152004** in aqueous solution had been studied in distilled water using a high-pressure mercury lamp and a xenon lamp as light source. The results of photodynamic experiments showed that **IPP152001** and **IPPA152004** in aqueous solution followed pseudo-first-order kinetics. Compared with imidacloprid, the order of photodegradation of these compounds was as follows: imidacloprid > **IPP152001** ≥ **IPPA152004-2** ≥ **IPPA152004-1**. The introduction of a tetrahydropyridine ring into NTN32692 was beneficial to increase the

photostability of nitromethylene analogues of imidacloprid. Moreover, there is a difference between the photodegradation rate of a pair of epimers. Using GC-MS, LC-TOF-MS with ESI positive mode, and LC-MS/MS, photodegradation products of **IPPA152004** had been preliminarily identified, and a possible explanation of the photodegradation pathways of **IPPA152004** was also proposed. The photodegradation pathways of **IPPA152004** were partially in accordance with the traditional degradation pathway of imidacloprid, whereas the main photolysis was different. Consequently, the main photochemical process occurred on the tetrahydropyridine ring, including elimination of nitro and photooxidation.

#### ACKNOWLEDGMENT

We are grateful to the school of Pharmacy of East China University of Science and Technology, Dr. Feifang Zhang, and Hui Shi for assistance in the LC-MS/MS analysis.

**Supporting Information Available:** Total ion chromatograms and ESI/MS spectra of the photoproducts of **IPPA152004** by analysis of LC-MS and GC-MS. This material is available free of charge via the Internet at <http://pubs.acs.org>.

#### LITERATURE CITED

- Burkhard, N.; Guth, J. A. Photolysis of organophosphorus insecticides on soil surfaces. *Pestic. Sci.* **1979**, *10*, 313–319.
- Guerard, J. J.; Chin, Y. P.; Mash, H.; Hadad, C. M. Photochemical fate of sulfadimethoxine in aquaculture waters. *Environ. Sci. Technol.* **2009**, *43*, 8587–8592.
- Chen, C.; Yang, S. G.; Guo, Y. P.; Sun, C.; Gu, C. G.; Xu, B. Photolytic destruction of endocrine disruptor atrazine in aqueous solution under UV irradiation: products and pathways. *J. Hazard. Mater.* **2009**, *172*, 675–684.
- Jackson, D. A.; Mabury, S. A. Environmental properties of pentafluorosulfanyl compounds: physical properties and photodegradation. *Environ. Toxicol. Chem.* **2009**, *28*, 1866–1873.
- Xu, B. B.; Chen, Z. L.; Qi, F.; Shen, J. M.; Wu, F. C. Factors influencing the photodegradation of *N*-nitrosodimethylamine in drinking water. *Front. Environ. Sci. Eng. China* **2009**, *3*, 91–97.
- Shiokawa, K.; Tsuboi, S.; Kagabu, S.; Moriya, K. *Heterocyclic compounds*. Eur. Pat. Appl. 0192060, 1986.
- Jeschkel, P.; Nauen, R. Neonicotinoids—from zero to hero in insecticide chemistry. *Pest Manag. Sci.* **2008**, *64*, 1084–1098.
- Wamhoff, H.; Schneider, V. Photodegradation of imidacloprid. *J. Agric. Food Chem.* **1999**, *47*, 1730–1734.
- Moza, P. N.; Justert, K.; Feicht, E.; Kettrup, A. Photolysis of imidacloprid in aqueous solution. *Chemosphere* **1998**, *36*, 497–502.
- de Urzedo, A. P. F. M.; Diniz, M. E. R.; Nascentes, C. C. Photolytic degradation of the insecticide thiamethoxam in aqueous medium monitored by direct infusion electrospray ionization mass spectrometry. *J. Mass Spectrom.* **2007**, *42*, 1319–1325.
- Redlich, D.; Shahin, N.; Ekici, P.; Friess, A.; Parlar, H. Kinetic study of the photoinduced degradation of imidacloprid in aquatic media. *Clean* **2007**, *35*, 452–458.
- Suman, G.; Gajbhiye, V. T.; Gupta, R. K. Effect of light on the degradation of two neonicotinoids viz acetamiprid and thiacloprid in soil. *Bull. Environ. Contam. Toxicol.* **2008**, *81*, 185–189.
- Liu, W. P.; Zheng, W.; Ma, Y.; Liu, K. K. Sorption and degradation of imidacloprid in soil and water. *J. Environ. Sci. Health B* **2006**, *41*, 623–634.
- Malato, S.; Caceres, J.; Aguera, A.; Mezcuca, M.; Hernando, D.; Vial, J.; Fernandez-Alba, A. R. Degradation of imidacloprid in water by photo-Fenton and TiO<sub>2</sub> photocatalysis at a solar pilot plant: a comparative study. *Environ. Sci. Technol.* **2001**, *35*, 4359–4366.
- Černigoj, U.; Štangar, L. U.; Trebše, P. Degradation of neonicotinoid insecticides by different advanced oxidation processes and studying the effect of ozone on TiO<sub>2</sub> photocatalysis. *Appl. Catal., B* **2007**, *75*, 229–238.
- Zheng, W.; Liu, W. P.; Wen, Y. Z.; Lee, S. J. Photochemistry of insecticide Imidacloprid: direct and sensitized photolysis in aqueous medium. *J. Environ. Sci.* **2004**, *16*, 539–542.
- Schippers, N.; Schwack, W. G. Photochemistry of imidacloprid in model systems. *J. Agric. Food Chem.* **2008**, *56*, 8023–8029.
- Kagabu, S.; Matsuno, H. Chloronicotinyl insecticides. 8. Crystal and molecular structures of imidacloprid and analogous compounds. *J. Agric. Food Chem.* **1997**, *45*, 276–281.
- Hilmar, W. L.; Benedikt, B. M.; Bemhard, H. L.; Wilhelm, S. W. *1,2,3,6-Tetrahydro-5-nitro-pyrimidin-derivates*. U.S. Patent 4,831,036, May 18, 1987.
- Tian, Z. Z.; Jiang, Z. X.; Song, G. H.; Huang, Q. C. Syntheses and biological activities of octahydro-1*H*-cyclopenta[*d*]pyrimidine derivatives. *J. Agric. Food Chem.* **2007**, *55*, 143–147.
- Li, Z.; Qian, X. H.; Shao, X. X.; Xu, X. Y.; Tian, Z. Z.; Huang, Q. C. *Preparation method and use of compounds having high insecticidal activities*. U.S. Patent 0,111,847, April 30, 2009.
- Xu, X.; Bao, H.; Shao, X.; Zhang, Y.; Yao, X.; Liu, Z.; Li, Z. Pharmacological characterization of cis-nitromethylene neonicotinoids in relation to imidacloprid binding sites in the brown planthopper, *Nilaparvata lugens*. *Insect Mol. Biol.* **2010**, 1–8.
- Elbert, A.; Nauen, R. Resistance of *Bemisia tabaci* (Homoptera Aleyrodidae) to insecticides in southern Spain with special reference to neonicotinoids. *Pest Manag. Sci.* **2000**, *56*, 60–64.
- Wang, Y. H.; Chen, J.; Zhu, Y.; Ma, C. Y.; Huang, Y.; Shen, J. L. Susceptibility to neonicotinoids and risk of resistance development in the brown planthopper, *Nilaparvata lugens* (Stål) (Homoptera: Delphacidae). *Pest Manag. Sci.* **2008**, *64*, 1278–1284.
- Shao, X. S.; Zhang, W. W.; Peng, Y. Q.; Li, Z.; Tian, Z. Z.; Qian, X. H. *cis*-Nitromethylene neonicotinoids as new nicotinic family: synthesis, structural diversity, and insecticidal evaluation of hexahydroimidazo[1,2- $\alpha$ ]pyridine. *Bioorg. Med. Chem. Lett.* **2008**, *18*, 6513–6516.
- Hatchard, C. G.; Parker, C. A. A new sensitive chemical actinometer. II. Potassium ferrioxalate as a standard chemical actinometer. *Proc. R. Soc. London, Ser. A* **1956**, *235*, 518–536.
- Vilhunen, S. H.; Sillanpää, M. E. Ultraviolet light emitting diodes and hydrogen peroxide in the photodegradation of aqueous phenol. *J. Hazard. Mater.* **2009**, *161*, 1530–1534.
- Leifer, A. *The Kinetics of Environmental Aquatic Photochemistry*; American Chemical Society: Washington, DC, 1988; pp 148–150.
- Kagabu, S.; Medej, S. Stability comparison of imidacloprid and related compounds under simulated sunlight, hydrolysis conditions, and oxygen. *Biosci., Biotechnol., Biochem.* **1995**, *59*, 980–985.
- Mielcarek, J.; Osmalek, T.; Kruszynska, M. Photodegradation products of new dihydropyridine derivatives. *Chromatographia* **2009**, *69*, 503–506.
- Li, Z.; Qian, X. H.; Shao, X. X.; Xu, X. Y.; Tian, Z. Z.; Huang, Q. C. *Preparation method and use of compounds having high insecticidal activities*. PCT/CN2006/00360, March 9, 2006.

---

Received for review July 31, 2009. Revised manuscript received December 15, 2009. Accepted December 16, 2009. This work was financially supported by National Basic Research Program of China (973 Program, 2003CB114405). This work was also partly supported by the grant “Application of Nuclear Techniques in Agriculture” from the Chinese Ministry of Agriculture (Grant 200803034), Shanghai Leading Academic Discipline Project, Project B507. 111 Project (No. B07023), and Program for New Century Excellent Talents in University (NCET070284).